Hindawi Publishing Corporation
EURASIP Journal on Wireless Communications and Networking
Volume 2007, Article ID 53742, 8 pages
doi:10.1155/2007/53742

Research Article

Error Probability of Binary and M-ary Signals with Spatial Diversity in Nakagami-q (Hoyt) Fading Channels

Trung Q. Duong, Hyundong Shin, and Een-Kee Hong

School of Electronics and Information, Kyung Hee University, 1 Seocheon-dong, Giheung-gu, Yongin-si, Gyeonggi-do 446-701, South Korea

Received 21 June 2007; Accepted 30 October 2007

Recommended by Ibrahim Develi

We analyze the exact average symbol error probability (SEP) of binary and M-ary signals with spatial diversity in Nakagami-q (Hoyt) fading channels. The maximal-ratio combining and orthogonal space-time block coding are considered as diversity techniques for single-input multiple-output and multiple-input multiple-output systems, respectively. We obtain the average SEP in terms of the Lauricella multivariate hypergeometric function $F_D^{(n)}$. The analysis is verified by comparing with Monte Carlo simulations and we further show that our general SEP expressions particularize to the previously known results for Rayleigh ($q = 1$) and single-input single-output (SISO) Nakagami-q cases.

1. INTRODUCTION

In digital communications, the accurate calculation of average symbol error probability (SEP) for a variety of modulation schemes has been an area of long-time interest (see [1–12] and references therein). A unified method for deriving the error probability over fading channels has been presented by using alternative representation of the Gaussian and Marcum Q-function [1, 2]. By their alternative representations, the average error probability can be expressed in the form of a single finite-range integral whose integrand contains the moment generation function (MGF) of instantaneous signal-to-noise ratio (SNR). In particular, closed-form solutions for average SEP of binary and M-ary modulations in Nakagami-m fading with positive integer m have been reported in [3]. More generally, the closed-form expressions for average SEP in Nakagami-m with arbitrary real-valued m have been derived in [4] and their extensions to single-input multiple-output (SIMO) diversity have been presented in [5, 6]. For multiple-input multiple-output (MIMO) diversity systems, the exact SEPs of orthogonal space-time block codes (OSTBCs) [13, 14] have been derived in [10–12] for Rayleigh, Rayleigh keyhole, Nakagami-m keyhole, and Rayleigh double-scattering MIMO channels, respectively.

In addition to Nakagami-m and Rayleigh fading, Nakagami-q fading, also referred to as Hoyt fading, has been considered recently in [15–17]. For example, average SEP of equal-gain combining (EGC) under the Hoyt model has been approximated in [15]. Also, the second-order statistics of maximal-ratio combining (MRC) and EGC in Nakagami-q fading have been studied in [16]. In addition, the level-crossing rate and the average duration of fades for Nakagami-q fading channels have been investigated in [17]. More recently, the performance of M-ary signallings for SISO Nakagami-q has been derived in [18].

In this paper, using the MGF-based method [1, 2] and transforming a single integral into the hypergeometric function [4], we derive the exact SEP expressions for spatial diversity systems in Nakagami-q fading. The final expressions are given in terms of Lauricella hypergeometric function $F_D^{(n)}$. It is further shown that the derived expressions reduce to the previously known results for Rayleigh fading ($q = 1$) and SISO Nakagami-q as special cases.

This paper is organized as follows. In Section 2, the statistical properties of the channel model are given. We then derive the exact average SEP for a broad class of binary and M-ary signals with MRC over SIMO Nakagami-q channels in Section 3. Section 4 gives the average SEP for OSTBCs over MIMO Nakagami-q channels. Numerical and simulation results are presented in Section 5. Finally, we conclude the paper in Section 6.

2. CHANNEL MODEL

The Nakagami-q fading spans from one-sided Gaussian fading ($q = 0$) to Rayleigh fading ($q = 1$), and is used to model fading environments more severe than Rayleigh fading—satellite communication links subject to strong ionospheric scintillation, for example. Assume that the transmitted signal is received over slowly varying SISO flat-fading channels. Let γ denote the instantaneous symbol SNR defined by

$$\gamma \triangleq \alpha^2 \frac{E_s}{N_0}, \tag{1}$$

where α is the fading amplitude, E_s the energy per symbol, and N_0 the one-sided power spectral density of additive white Gaussian noise (AWGN).

For Nakagami-q fading, the probability density function (pdf) of α with mean-square value $\Omega \triangleq \mathbb{E}\{\alpha^2\}$ is given by [1, 2]

$$\begin{aligned} p_\alpha(\alpha) = {} & \frac{(1+q^2)\alpha}{q\Omega} \exp\left(-\frac{(1+q^2)^2\alpha^2}{4q^2\Omega}\right) \\ & \times I_0\left(\frac{(1-q^4)\alpha^2}{4q^2\Omega}\right), \quad \alpha \geq 0, \end{aligned} \tag{2}$$

where $q \in [0, 1]$ is the fading severity parameter and $I_0(\cdot)$ is the zeroth-order modified Bessel function of the first kind. The pdf and MGF of γ are then given by [1, 2]

$$\begin{aligned} p_\gamma(\gamma) = {} & \frac{(1+q^2)}{2q\overline{\gamma}} \exp\left(-\frac{(1+q^2)^2\gamma}{4q^2\overline{\gamma}}\right) \\ & \times I_0\left(\frac{(1-q^4)\gamma}{4q^2\overline{\gamma}}\right), \quad \gamma \geq 0, \\ \phi_\gamma(s) \triangleq {} & \mathbb{E}\{e^{-s\gamma}\} = \left[\left(1+\frac{2s\overline{\gamma}}{1+q^2}\right)\left(1+\frac{2s\overline{\gamma}q^2}{1+q^2}\right)\right]^{-1/2}, \end{aligned} \tag{3}$$

where $\overline{\gamma} = \Omega E_s/N_0$ is the average SNR per symbol.

3. AVERAGE SEP FOR SIMO MRC

Assume that the transmitted signal is received over L-branch independent SIMO flat-fading channels. Then instantaneous SNR at the MRC output is given by

$$\gamma_{\text{MRC}} = \sum_{i=1}^{L} \alpha_i^2 \frac{E_s}{N_0}, \tag{4}$$

where α_i, $i = 1, 2, \ldots, L$ is the fading amplitude of the ith branch Nakagami-q fading channel with fading severity parameter q_i and mean-square value $\Omega_i = \mathbb{E}\{\alpha_i^2\}$.

Let $\gamma_i \triangleq \alpha_i^2 E_s/N_0$ denote the instantaneous SNR of the ith diversity branch. Then from statistical independence of α_i's, the MGF of MRC output SNR γ_{MRC} is given by

$$\begin{aligned} \phi_{\gamma_{\text{MRC}}}(s) = {} & \prod_{i=1}^{L} \phi_{\gamma_i}(s) \\ = {} & \prod_{i=1}^{L} \left[\left(1+\frac{2s\overline{\gamma}_i}{1+q_i^2}\right)\left(1+\frac{2s\overline{\gamma}_i q_i^2}{1+q_i^2}\right)\right]^{-1/2}, \end{aligned} \tag{5}$$

where $\overline{\gamma}_i = \Omega_i E_s/N_0$ denotes the average symbol SNR of the ith diversity branch. From the MGF of γ_{MRC}, we can evaluate the average SEP for a broad class of binary and M-ary signals over SIMO Nakagami-q channels by using a well-known MGF-based approach [1, 2].

3.1. M-ary phase-shift keying (M-PSK)

For coherent M-PSK, the average SEP can be written as [1–4]

$$\begin{aligned} P_{\text{e,MPSK}}^{\text{MRC}} = {} & \underbrace{\frac{1}{\pi}\int_0^{\pi/2} \phi_{\gamma_{\text{MRC}}}\left(\frac{g_1}{\sin^2\theta}\right)d\theta}_{\triangleq \mathcal{I}_{1,\text{MPSK}}} \\ & + \underbrace{\frac{1}{\pi}\int_{\pi/2}^{\pi-\pi/M} \phi_{\gamma_{\text{MRC}}}\left(\frac{g_1}{\sin^2\theta}\right)d\theta}_{\triangleq \mathcal{I}_{2,\text{MPSK}}}, \end{aligned} \tag{6}$$

where

$$g_1 = \sin^2\left(\frac{\pi}{M}\right). \tag{7}$$

By making the change of the variable $t = \cos^2\theta$ for $\mathcal{I}_{1,\text{MPSK}}$ and $t = \cos^2\theta/\cos^2(\pi/M)$ for $\mathcal{I}_{2,\text{MPSK}}$ [4], we have

$$\begin{aligned} \mathcal{I}_{1,\text{MPSK}} = {} & \frac{\phi_{\gamma_{\text{MRC}}}(g_1)}{2\pi}\int_0^1 t^{-1/2}(1-t)^{L-1/2} \\ & \times \prod_{i=1}^{L}\left(1-t\eta_{g_1}^{(i)}\right)^{-1/2}\left(1-t\zeta_{g_1}^{(i)}\right)^{-1/2}dt, \\ \mathcal{I}_{2,\text{MPSK}} = {} & \frac{\sqrt{g_2}\phi_{\gamma_{\text{MRC}}}(g_1)}{2\pi}\int_0^1 t^{-1/2}(1-tg_2)^{L-1/2} \\ & \times \prod_{i=1}^{L}\left(1-tg_2\eta_{g_1}^{(i)}\right)^{-1/2}\left(1-tg_2\zeta_{g_1}^{(i)}\right)^{-1/2}dt, \end{aligned} \tag{8}$$

where

$$\begin{aligned} g_2 = {} & \cos^2\left(\frac{\pi}{M}\right), \\ \eta_g^{(i)} = {} & \left(1+\frac{2g\overline{\gamma}_i}{1+q_i^2}\right)^{-1}, \\ \zeta_g^{(i)} = {} & \left(1+\frac{2g\overline{\gamma}_i q_i^2}{1+q_i^2}\right)^{-1}. \end{aligned} \tag{9}$$

Note that the integrals in (8) can be expressed in terms of Lauricella multivariate hypergeometric function $F_D^{(n)}$ whose Euler integral representation is given by [19, equation (2.3.6)]

$$\begin{aligned} & F_D^{(n)}(a, \{b_i\}_{i=1}^n; c; \{x_i\}_{i=1}^n) \\ & \quad = \frac{\Gamma(c)}{\Gamma(a)\Gamma(c-a)}\int_0^1 t^{a-1}(1-t)^{c-a-1}\prod_{i=1}^{n}(1-x_i t)^{-b_i}dt, \\ & \max\{|x_1|, |x_2|, \ldots, |x_n|\} < 1, \quad \text{Re}(c) > \text{Re}(a) > 0, \end{aligned} \tag{10}$$

where $\Gamma(\cdot)$ is Euler gamma function. Note that $F_D^{(1)}$ and $F_D^{(2)}$ reduce to the Gauss hypergeometric function ${}_2F_1(a, b; c; z)$

[20, equation 2.12(1)] and the Appell hypergeometric function $F_1(a,b,b';c;x,y)$ [20, equation 5.8(5)], respectively. Evaluating (8) in terms of Lauricella hypergeometric functions $F_D^{(2L)}$ and $F_D^{(2L+1)}$, we obtain the average SEP for M-PSK signals over Nakagami-q fading channels with L-branch MRC as

$$\begin{aligned}P_{\text{e,MPSK}}^{\text{MRC}} &= \frac{\Gamma(L+1/2)}{2\sqrt{\pi}\Gamma(L+1)}\phi_{\gamma_{\text{MRC}}}(g_1)\\ &\times F_D^{(2L)}\left(\frac{1}{2},\underbrace{\frac{1}{2},\ldots,\frac{1}{2}}_{2L};L+1;\right.\\ &\qquad\left.\left\{\eta_{g_1}^{(i)}\right\}_{i=1}^{L},\left\{\zeta_{g_1}^{(i)}\right\}_{i=1}^{L}\right)+\frac{\sqrt{g_2}}{\pi}\phi_{\gamma_{\text{MRC}}}(g_1)\\ &\times F_D^{(2L+1)}\left(\frac{1}{2},\underbrace{\frac{1}{2},\ldots,\frac{1}{2}}_{2L},-L+\frac{1}{2};\frac{3}{2};\right.\\ &\qquad\left.\left\{g_2\eta_{g_1}^{(i)}\right\}_{i=1}^{L},\left\{g_2\zeta_{g_1}^{(i)}\right\}_{i=1}^{L},g_2\right).\end{aligned} \tag{11}$$

For $M=2$ (binary PSK), $\mathcal{I}_{2,\text{MPSK}}$ (or equivalently the second term of (11)) is equal to zero. Hence, the average bit error probability (BEP) for binary PSK with MRC in Nakagami-q fading becomes the first term of (11) with $g_1=1$.

Special cases

(i) Independent and identically distributed (i.i.d.) SIMO Nakagami-q fading channel ($q_i=q$ and $\Omega_i=\Omega$, $i=1,2,\ldots,L$): with the help of the reduction formula (A.1) in the appendix, (11) reduces to

$$\begin{aligned}P_{\text{e,MPSK}}^{\text{MRC}} &= \frac{\Gamma(L+1/2)\phi_{\gamma_{\text{MRC}}}(g_1)}{2\sqrt{\pi}\Gamma(L+1)}\\ &\times F_1\left(\frac{1}{2},\frac{L}{2},\frac{L}{2};L+1;\eta_{g_1}^{\star},\zeta_{g_1}^{\star}\right)+\frac{\sqrt{g_2}\phi_{\gamma_{\text{MRC}}}(g_1)}{\pi}\\ &\times F_D^{(3)}\left(\frac{1}{2},\frac{L}{2},\frac{L}{2},-L+\frac{1}{2};\frac{3}{2};g_2\eta_{g_1}^{\star},g_2\zeta_{g_1}^{\star},g_2\right),\end{aligned} \tag{12}$$

where

$$\eta_g^{\star}=\left(1+\frac{2g\bar{\gamma}}{1+q^2}\right)^{-1},\qquad \zeta_g^{\star}=\left(1+\frac{2g\bar{\gamma}q^2}{1+q^2}\right)^{-1}. \tag{13}$$

(ii) SISO Nakagami-q fading channel ($L=1$): substituting $L=1$ into (12) and noting that for $n=2$, $F_D^{(n)}(\cdot)$ reduces to $F_1(\cdot)$, we obtain the same result as in [18, equation (18)].

(iii) Rayleigh fading channel with L-branch MRC ($q_i=1$): substituting $q=1$ into (12), we have $\eta_{g_1}^{\star}=\zeta_{g_1}^{\star}$, leading to the same result as in [5, equation (7)] for Rayleigh fading ($m=1$) with again the help of (A.1).

(iv) SISO Rayleigh fading channel ($L=1$ and $q=1$): substituting $q=1$ and $L=1$ into (12), we obtain the same result as in [4, equation (10)] for Rayleigh fading ($m=1$), which further reduces to [2, equation (8.112)] in terms of elementary functions (see [4] for details).

3.2. M-ary quadrature amplitude modulation (M-QAM)

For coherent square M-QAM, the average SEP is given by [1–4]

$$\begin{aligned}P_{\text{e,MQAM}}^{\text{MRC}} &= \underbrace{\frac{4g_4}{\pi}\int_0^{\pi/2}\phi_{\gamma_{\text{MRC}}}\left(\frac{g_3}{\sin^2\theta}\right)d\theta}_{\triangleq\mathcal{I}_{1,\text{MQAM}}}\\ &\quad-\underbrace{\frac{4g_4^2}{\pi}\int_0^{\pi/4}\phi_{\gamma_{\text{MRC}}}\left(\frac{g_3}{\sin^2\theta}\right)d\theta}_{\triangleq\mathcal{I}_{2,\text{MQAM}}},\end{aligned} \tag{14}$$

where

$$g_3=\frac{3}{2(M-1)},\qquad g_4=1-\frac{1}{\sqrt{M}}. \tag{15}$$

Considering the similarity of $\mathcal{I}_{1,\text{MQAM}}$ to $\mathcal{I}_{1,\text{MPSK}}$ and making the change of variable $t=1-\tan^2\theta$ in $\mathcal{I}_{2,\text{MQAM}}$ (after some manipulations) [4], we obtain the average SEP for M-QAM signals over Nakagami-q fading channels with L-branch MRC as

$$\begin{aligned}P_{\text{e,MQAM}}^{\text{MRC}} &= \frac{2g_4\Gamma(L+1/2)}{\sqrt{\pi}\Gamma(L+1)}\phi_{\gamma_{\text{MRC}}}(g_3)\\ &\times F_D^{(2L)}\left(\frac{1}{2},\underbrace{\frac{1}{2},\ldots,\frac{1}{2}}_{2L};L+1;\left\{\eta_{g_3}^{(i)}\right\}_{i=1}^{L},\left\{\zeta_{g_3}^{(i)}\right\}_{i=1}^{L}\right)\\ &-\frac{2g_4^2}{\pi(1+2L)}\phi_{\gamma_{\text{MRC}}}(2g_3)\\ &\times F_D^{(2L+1)}\left(1,\underbrace{\frac{1}{2},\ldots,\frac{1}{2}}_{2L},1;L+\frac{3}{2};\right.\\ &\qquad\left.\left\{\frac{\eta_{2g_3}^{(i)}}{\eta_{g_3}^{(i)}}\right\}_{i=1}^{L},\left\{\frac{\zeta_{2g_3}^{(i)}}{\zeta_{g_3}^{(i)}}\right\}_{i=1}^{L},\frac{1}{2}\right).\end{aligned} \tag{16}$$

Special cases

(i) I.I.D. SIMO Nakagami-q fading channel ($q_i=q$ and $\Omega_i=\Omega$, $i=1,2,\ldots,L$): with the help of (A.1), (16) reduces to

$$\begin{aligned}P_{\text{e,MQAM}}^{\text{MRC}} &= \frac{2g_4\Gamma(L+1/2)\phi_{\gamma_{\text{MRC}}}(g_3)}{\sqrt{\pi}\Gamma(L+1)}\\ &\times F_1\left(\frac{1}{2},\frac{L}{2},\frac{L}{2};L+1;\eta_{g_3}^{\star},\zeta_{g_3}^{\star}\right)\\ &-\frac{2g_4^2\phi_{\gamma_{\text{MRC}}}(2g_3)}{\pi(1+2L)}\\ &\times F_D^{(3)}\left(1,\frac{L}{2},\frac{L}{2},1;L+\frac{3}{2};\frac{\eta_{2g_3}^{\star}}{\eta_{g_3}^{\star}},\frac{\zeta_{2g_3}^{\star}}{\zeta_{g_3}^{\star}},\frac{1}{2}\right).\end{aligned} \tag{17}$$

(ii) SISO Nakagami-q fading channel ($L = 1$): substituting $L = 1$ into (17), we obtain the same result as in [18, equation (21)].

(iii) Rayleigh fading channel with L-branch MRC ($q_i = 1$): substituting $q = 1$ into (17), we have $\eta_{g_3}^{\star} = \zeta_{g_3}^{\star}$ and $\eta_{2g_3}^{\star} = \zeta_{2g_3}^{\star}$, leading to the same result as in [5, equation (12)] for Rayleigh fading ($m = 1$) with again the help of (A.1).

(iv) SISO Rayleigh fading channel ($L = 1$ and $q = 1$): substituting $q = 1$ and $L = 1$ into (17), we obtain the same result as in [4, equation (12)] for Rayleigh fading ($m = 1$), which further reduces to [2, equation (8.106)] in terms of elementary functions (see [4] for details).

3.3. M-ary differential PSK (M-DPSK)

The average SEP for differentially coherent detection of M-DPSK signals is given by [1–4]

$$P_{\mathrm{e,MDPSK}}^{\mathrm{MRC}} = \frac{1}{\pi}\int_0^{\pi-\pi/M} \phi_{\gamma_{\mathrm{MRC}}}\left(\frac{g_1}{1+\sqrt{g_2}+\cos\theta}\right)d\theta. \tag{18}$$

Letting

$$g_5 = 2\sin^2\left(\frac{\pi}{2M}\right), \qquad g_6 = \cos^2\left(\frac{\pi}{2M}\right), \tag{19}$$

and making the change of the variable [4]

$$t = \frac{\sin^2\theta}{\sin^2(\pi/2-\pi/2M)}, \tag{20}$$

equation (18) can be evaluated (after some algebra) as

$$P_{\mathrm{e,MDPSK}}^{\mathrm{MRC}} = \frac{2\sqrt{g_6}}{\pi}\phi_{\gamma_{\mathrm{MRC}}}(g_5)F_D^{(2L+2)} \times F_D^{(2L+2)}\left(\frac{1}{2},\underbrace{\frac{1}{2},\ldots,\frac{1}{2}}_{2L},-L,\frac{1}{2};\frac{3}{2};\left\{\sqrt{g_2}\eta_{g_5}^{(i)}\right\}_{i=1}^{L},\left\{\sqrt{g_2}\zeta_{g_5}^{(i)}\right\}_{i=1}^{L},\sqrt{g_2},g_6\right). \tag{21}$$

Special cases

(i) I.I.D. SIMO Nakagami-q fading channel ($q_i = q$ and $\Omega_i = \Omega$, $i = 1, 2, \ldots, L$): with the help of (A.1), (21) reduces to

$$P_{\mathrm{e,MDPSK}}^{\mathrm{MRC}} = \frac{2\sqrt{g_6}\phi_{\gamma_{\mathrm{MRC}}}(g_5)}{\pi} \times F_D^{(4)}\left(\frac{1}{2},\frac{L}{2},\frac{L}{2},\frac{L}{2},-L,\frac{1}{2};\frac{3}{2};\sqrt{g_2}\eta_{g_5}^{\star},\sqrt{g_2}\zeta_{g_5}^{\star},\sqrt{g_2},g_6\right). \tag{22}$$

(ii) SISO Nakagami-q fading channel ($L = 1$): substituting $L = 1$ into (22), we obtain the same result as in [18, equation (10)] for SISO Nakagami-q fading with again the help of (A.1).

(iii) Rayleigh fading channel with L-branch MRC ($q_i = 1$): substituting $q = 1$ into (22), we have $\eta_{g_5}^{\star} = \zeta_{g_5}^{\star}$, leading to the same result as in [5, equation (14)] for Rayleigh fading ($m = 1$) with again the help of (A.1).

(iv) SISO Rayleigh fading channel ($L = 1$ and $q = 1$): substituting $q = 1$ and $L = 1$ into (22), we obtain the same result as in [4, equation (14)] for Rayleigh fading ($m = 1$), which further reduces to [9, equation (8)] in terms of elementary functions (see [4] for details).

3.4. Noncoherent correlated binary signals and $\pi/4$-differential quaternary PSK (DQPSK)

The average BEP for equal energy, equiprobable, correlated binary signals with noncoherent detection is given by [1–4]

$$P_{\mathrm{b,NCB}}^{\mathrm{MRC}} = \frac{1}{2\pi}\int_0^{\pi} \phi_{\gamma_{\mathrm{MRC}}}\left(\frac{\left(v^2-u^2\right)^2}{2(u+v)^2-4uv\cos\theta}\right)d\theta \tag{23}$$

with

$$u = \left(\frac{1-\sqrt{1-|\rho|^2}}{2}\right)^{1/2}, \qquad v = \left(\frac{1+\sqrt{1-|\rho|^2}}{2}\right)^{1/2}, \tag{24}$$

where $|\rho| \in [0, 1]$ is the magnitude of cross correlation coefficient between two signals. Note that the special case of $\rho = 0$ (i.e., $u = 0$ and $v = 1$) corresponds to noncoherent orthogonal binary frequency-shift keying (FSK).

Letting

$$g_7 = \frac{(v-u)^2}{2}, \qquad g_8 = \frac{4uv}{(u+v)^2}, \tag{25}$$

and making the change of the variable $t = \cos^2\theta$ [4], (23) can be evaluated (after some algebra) as

$$P_{\mathrm{b,NCB}}^{\mathrm{MRC}} = \frac{1}{2}\phi_{\gamma_{\mathrm{MRC}}}(g_7)F_D^{(2L+1)}\left(\frac{1}{2},\underbrace{\frac{1}{2},\ldots,\frac{1}{2}}_{2L},-L;1;\left\{g_8\eta_{g_7}^{(i)}\right\}_{i=1}^{L},\left\{g_8\zeta_{g_7}^{(i)}\right\}_{i=1}^{L},g_8\right). \tag{26}$$

Since $u = \sqrt{2-\sqrt{2}}$ and $v = \sqrt{2+\sqrt{2}}$ correspond to $\pi/4$-DQPSK with Gray coding [1–4], we can obtain the average SEP for $\pi/4$-DQPSK directly from (26) with these particular values of u and v (or equivalently $g_7 = 2-\sqrt{2}$ and $g_8 = 2\sqrt{2}/(2+\sqrt{2})$).

Special cases

(i) I.I.D. SIMO Nakagami-q fading channel ($q_i = q$ and $\Omega_i = \Omega$, $i = 1, 2, \ldots, L$): with the help of (A.1), (26) reduces to

$$P_{\mathrm{b,NCB}}^{\mathrm{MRC}} = \frac{\phi_{\gamma_{\mathrm{MRC}}}(g_7)}{2} \times F_D^{(3)}\left(\frac{1}{2},\frac{L}{2},\frac{L}{2},-L;1;g_8\eta_{g_7}^{\star},g_8\zeta_{g_7}^{\star},g_8\right). \tag{27}$$

In particular, (27) for $L = 1$ (SISO Nakagami-q fading) reduces (with the help of the reduction formula (A.2) in the appendix) to

$$P_{\mathrm{b,NCB}} = \frac{\phi_\gamma(g_7)}{2} F_1\left(\frac{1}{2}, \frac{1}{2}, \frac{1}{2}; 1; g_8\eta^\star_{g_7}, g_8\zeta^\star_{g_7}\right) - \frac{g_8\phi_\gamma(g_7)}{4} F_1\left(\frac{3}{2}, \frac{1}{2}, \frac{1}{2}; 2; g_8\eta^\star_{g_7}, g_8\zeta^\star_{g_7}\right), \tag{28}$$

which agrees with [18, equation (15)].

(ii) Rayleigh fading channel with L-branch MRC ($q_i = 1$): substituting $q = 1$ into (27), we have $\eta^\star_{g_7} = \zeta^\star_{g_7}$, leading to the same result as in [5, equation (16)] for Rayleigh fading ($m = 1$) with again the help of (A.1).

(iii) SISO Rayleigh fading channel ($L = 1$ and $q = 1$): substituting $q = 1$ and $L = 1$ into (27), we obtain the same result as in [4, equation (7)] for Rayleigh fading ($m = 1$), which further reduces to [3, equation (22)] in terms of elementary functions (with the aid of identity [4, equation (19)]).

4. AVERAGE SEP FOR OSTBC

In this section, we extend the analysis to MIMO diversity systems employing an OSTBC for multiple transmit antennas [13, 14]. We consider a slowly varying, frequency-flat, Nakagami-q fading MIMO channel with n_t transmit and n_r receive antennas.

Let $\mathbf{H}$ be the $n_r \times n_t$ channel matrix whose (i, j)th entries h_{ij}, $i = 1, 2, \ldots, n_r$, $j = 1, 2, \ldots, n_t$, are statistically independent complex propagation coefficients between the jth transmit and the ith receive antennas. The fading amplitude $|h_{ij}|$ of the (i, j)th link is a Nakagami-q variable with fading severity parameter q_{ij} and $\mathbb{E}\{|h_{ij}|^2\} = \Omega_{ij}$.

4.1. MGF of output SNR

During a K-symbol interval, the $K \times n_t$ OSTBC $\mathcal{G}_{n_t}$ consisting of N symbols (M-PSK or M-QAM) $x_1, x_2, \ldots, x_N$ is transmitted with the rate $\mathcal{R} = N/K$, where the average energy of symbol transmitted from each antenna is normalized to be E_s/n_t. A general construction of complex OSTBCs with minimal delay and maximal achievable rate was presented in [21]. This construction of OSTBCs for n_t transmit antennas gives the maximal achievable rate [21, Theorem 1]

$$\mathcal{R} = \frac{\lceil \log_2 n_t \rceil + 1}{2^{\lceil \log_2 n_t \rceil}}, \tag{29}$$

where $\lceil x \rceil$ denotes the smallest integer greater than or equal to x. For example, one-rate Alamouti OSTBC $\mathcal{G}_2$ for two transmit antennas [13] and 3/4-rate OSTBC $\mathcal{G}_4$ for four transmit antennas [21] are given by

$$\mathcal{G}_2 = \begin{bmatrix} x_1 & x_2 \\ -x_2^* & x_1^* \end{bmatrix}, \qquad \mathcal{G}_4 = \begin{bmatrix} x_1 & x_2 & x_3 & 0 \\ -x_2^* & x_1^* & 0 & -x_3 \\ -x_3^* & 0 & x_1^* & x_2 \\ 0 & x_3^* & -x_2^* & x_1 \end{bmatrix}, \tag{30}$$

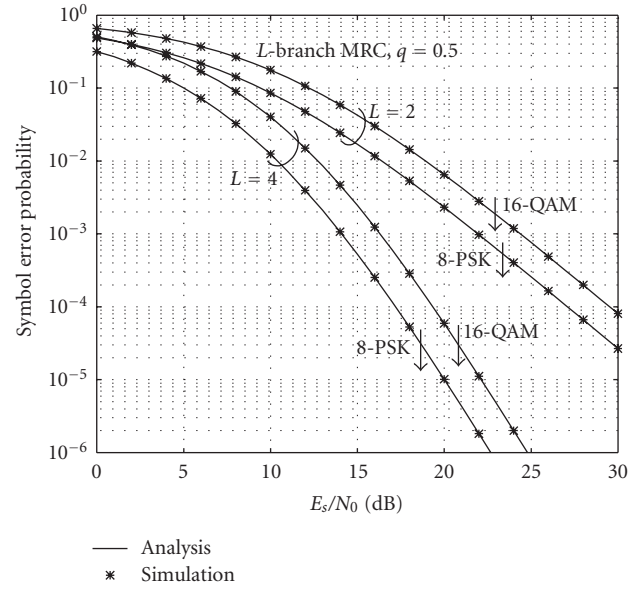

Figure 1: Symbol error probability of 8-PSK and 16-QAM versus E_s/N_0 for L-branch MRC in SIMO Nakagami-q fading channels. $q = 0.5$, $L = 2$ and 4.

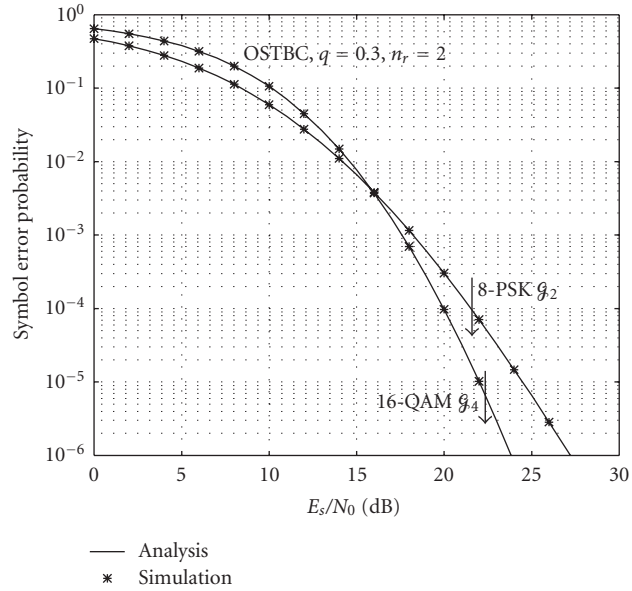

Figure 2: Symbol error probability of 8-PSK $\mathcal{G}_2$ and 16-QAM $\mathcal{G}_4$ OSTBCs (3 bits/s/Hz) versus E_s/N_0 in MIMO Nakagami-q fading channels. $q = 0.3$ and $n_r = 2$.

where the superscript $(\cdot)^*$ stands for the complex conjugate. It is well known that due to the unitary property of OSTBCs, the orthogonal space-time block encoding and decoding transform a MIMO channel into N equivalent SISO subchannels with a path gain of the Frobenius norm of $\mathbf{H}$, yielding instantaneous output symbol SNR for each of SISO subchannels [10, 11]

$$\gamma_{\mathrm{STBC}} = \frac{1}{n_t\mathcal{R}} \sum_{i=1}^{n_r} \sum_{j=1}^{n_t} |h_{ij}|^2 \frac{E_s}{N_0}. \tag{31}$$

Since all the h_{ij}'s are independent, the MGF of γ_{STBC} can be easily written as

$$\phi_{\gamma_{\text{STBC}}}(s) = \prod_{i=1}^{n_r}\prod_{j=1}^{n_t}\left[\left(1+\frac{2s\overline{\gamma}_{ij}/n_t\mathcal{R}}{1+q_{ij}^2}\right)\left(1+\frac{2s\overline{\gamma}_{ij}q_{ij}^2/n_t\mathcal{R}}{1+q_{ij}^2}\right)\right]^{-1/2}, \tag{32}$$

where $\overline{\gamma}_{ij} = \Omega_{ij}E_s/N_0$.

4.2. M-PSK and M-QAM

From analogy of the MGF of γ_{STBC} in (32) to (5), we can obtain the average SEPs for OSTBC with M-PSK and M-QAM immediately from (11) and (16) as follows:

$$\begin{aligned}
P_{\text{e,MPSK}}^{\text{STBC}} &= \frac{\Gamma(n_tn_r+1/2)}{2\sqrt{\pi}\Gamma(n_tn_r+1)}\phi_{\gamma_{\text{STBC}}}(g_1)\\
&\quad\times F_D^{(2n_tn_r)}\left(\frac{1}{2},\underbrace{\frac{1}{2},\ldots,\frac{1}{2}}_{2n_tn_r};n_tn_r+1;\left\{\eta_{\breve{g}_1}^{(ij)}\right\}_{\substack{1\le i\le n_r\\1\le j\le n_t}},\right.\\
&\qquad\left.\left\{\zeta_{\breve{g}_1}^{(ij)}\right\}_{\substack{1\le i\le n_r\\1\le j\le n_t}}\right)+\frac{\sqrt{g_2}}{\pi}\phi_{\gamma_{\text{STBC}}}(g_1)\\
&\quad\times F_D^{(2n_tn_r+1)}\left(\frac{1}{2},\underbrace{\frac{1}{2},\ldots,\frac{1}{2}}_{2n_tn_r},-n_tn_r+\frac{1}{2};\frac{3}{2};\right.\\
&\qquad\left.\left\{g_2\eta_{\breve{g}_1}^{(ij)}\right\}_{\substack{1\le i\le n_r\\1\le j\le n_t}},\left\{g_2\zeta_{\breve{g}_1}^{(ij)}\right\}_{\substack{1\le i\le n_r\\1\le j\le n_t}},g_2\right),\\
P_{\text{e,MQAM}}^{\text{STBC}} &= \frac{2g_4\Gamma(n_tn_r+1/2)}{\sqrt{\pi}\Gamma(n_tn_r+1)}\phi_{\gamma_{\text{STBC}}}(g_3)\\
&\quad\times F_D^{(2n_tn_r)}\left(\frac{1}{2},\underbrace{\frac{1}{2},\ldots,\frac{1}{2}}_{2n_tn_r};n_tn_r+1;\left\{\eta_{\breve{g}_3}^{(ij)}\right\}_{\substack{1\le i\le n_r\\1\le j\le n_t}},\right.\\
&\qquad\left.\left\{\zeta_{\breve{g}_3}^{(ij)}\right\}_{\substack{1\le i\le n_r\\1\le j\le n_t}}\right)-\frac{2g_4^2\phi_{\gamma_{\text{STBC}}}(2g_3)}{\pi(1+2n_tn_r)}\\
&\quad\times F_D^{(2n_tn_r+1)}\left(1,\underbrace{\frac{1}{2},\ldots,\frac{1}{2}}_{2n_tn_r},1;n_tn_r+\frac{3}{2};\right.\\
&\qquad\left.\left\{\frac{\eta_{2\breve{g}_3}^{(ij)}}{\eta_{\breve{g}_3}^{(ij)}}\right\}_{\substack{1\le i\le n_r\\1\le j\le n_t}},\left\{\frac{\zeta_{2\breve{g}_3}^{(ij)}}{\zeta_{\breve{g}_3}^{(ij)}}\right\}_{\substack{1\le i\le n_r\\1\le j\le n_t}},\frac{1}{2}\right),
\end{aligned} \tag{33}$$

where $\breve{g}_1 = g_1/(n_t\mathcal{R})$ and $\breve{g}_3 = g_3/(n_t\mathcal{R})$.

Special cases

(i) I.I.D. MIMO Nakagami-q fading channel ($q_{ij} = q$ and $\Omega_{ij} = \Omega$, $i = 1,2,\ldots,n_r$, $j = 1,2,\ldots,n_t$): with the help of (A.1), (33) reduce to

$$\begin{aligned}
P_{\text{e,MPSK}}^{\text{STBC}} &= \frac{\Gamma(n_tn_r+1/2)\phi_{\gamma_{\text{STBC}}}(g_1)}{2\sqrt{\pi}\Gamma(n_tn_r+1)}\\
&\quad\times F_1\left(\frac{1}{2},\frac{n_tn_r}{2},\frac{n_tn_r}{2};n_tn_r+1;\eta_{\breve{g}_1}^{\star},\zeta_{\breve{g}_1}^{\star}\right)\\
&\quad+\frac{\sqrt{g_2}\phi_{\gamma_{\text{STBC}}}(g_1)}{\pi}\\
&\quad\times F_D^{(3)}\left(\frac{1}{2},\frac{n_tn_r}{2},\frac{n_tn_r}{2},-n_tn_r+\frac{1}{2};\frac{3}{2};g_2\eta_{\breve{g}_1}^{\star},g_2\zeta_{\breve{g}_1}^{\star},g_2\right),\\
P_{\text{e,MQAM}}^{\text{STBC}} &= \frac{2g_4\Gamma(n_tn_r+1/2)\phi_{\gamma_{\text{STBC}}}(g_3)}{\sqrt{\pi}\Gamma(n_tn_r+1)}\\
&\quad\times F_1\left(\frac{1}{2},\frac{n_tn_r}{2},\frac{n_tn_r}{2};n_tn_r+1;\eta_{\breve{g}_3}^{\star},\zeta_{\breve{g}_3}^{\star}\right)\\
&\quad-\frac{2g_4^2\phi_{\gamma_{\text{STBC}}}(2g_3)}{\pi(1+2n_tn_r)}\\
&\quad\times F_D^{(3)}\left(1,\frac{n_tn_r}{2},\frac{n_tn_r}{2},1;n_tn_r+\frac{3}{2};\frac{\eta_{2\breve{g}_3}^{\star}}{\eta_{\breve{g}_3}^{\star}},\frac{\zeta_{2\breve{g}_3}^{\star}}{\zeta_{\breve{g}_3}^{\star}},\frac{1}{2}\right),
\end{aligned} \tag{34}$$

respectively.

(ii) I.I.D. MIMO Rayleigh fading channel ($q_{ij} = 1$): substituting $q = 1$ into (34), we have $\eta_{\breve{g}_1}^{\star} = \zeta_{\breve{g}_1}^{\star}$, $\eta_{\breve{g}_3}^{\star} = \zeta_{\breve{g}_3}^{\star}$, and $\eta_{2\breve{g}_3}^{\star} = \zeta_{2\breve{g}_3}^{\star}$, leading to the same results as in [10, equations (23) and (24)] for Rayleigh fading ($m = 1$) with again the help of (A.1), which further reduce to [10, equations (26) and (27)] in terms of elementary functions.

5. NUMERICAL AND SIMULATION RESULTS

To validate our analysis, we perform Monte Carlo simulations and compare them with analytical results. For the simulation of Nakagami-q (Hoyt) fading model, the approximation of the Hoyt model by a properly chosen Nakagami-m model has been presented in [15]. In our examples, we obtain the Nakagami-q fading by taking account of the physical model of the λ-μ distribution [22]: $\mu = 0.5$ and $\lambda = (1-q^2)/(1+q^2)$. In such a case, the in-phase and quadrature components of the Nakagami-q fading envelope are modeled as the sum of several zero-mean correlated Gaussian random variables with a correlation coefficient $(1-q^2)/(1+q^2)$. In all examples (for brevity of simulations), we set $q_i = q$ and $\Omega_i = 1$, $i = 1,2,\ldots,L$ for SIMO Nakagami-q fading, and $q_{ij} = q$ and $\Omega_{ij} = 1$, $i = 1,2,\ldots,n_r$, $j = 1,2,\ldots,n_t$ for MIMO Nakagami-q fading. Hence, the average symbol SNR per receive antenna is equal to E_s/N_0.

Figure 1 shows the average SEP of 8-PSK and 16-QAM versus E_s/N_0 for L-branch MRC in SIMO Nakagami-q fading channels when $q = 0.5$, $L = 2$ and 4. Figure 2 shows the SEP of 8-PSK $\mathcal{G}_2$ and 16-QAM $\mathcal{G}_4$ OSTBCs versus E_s/N_0 in MIMO Nakagami-q fading channels when $q = 0.3$ and $n_r = 2$. For 8-PSK $\mathcal{G}_2$ and 16-QAM $\mathcal{G}_4$, the transmission rate is equal to

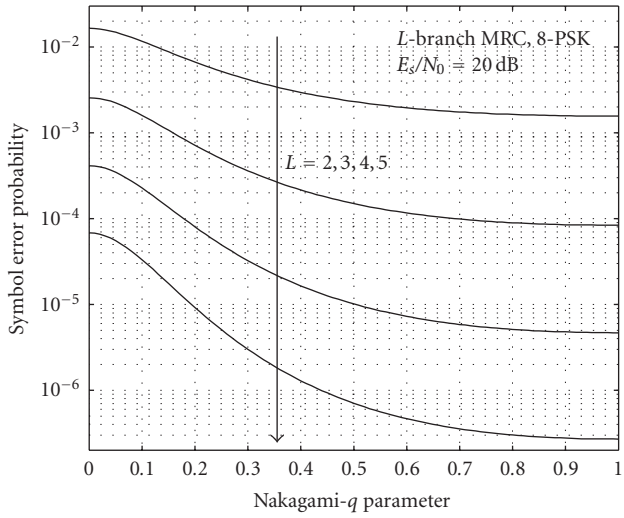

Figure 3: Symbol error probability of 8-PSK with L-branch MRC in SIMO Nakagami-q fading channels as a function of the Nakagami-q parameter. $L = 2, 3, 4, 5$ and $E_s/N_0 = 20$ dB.

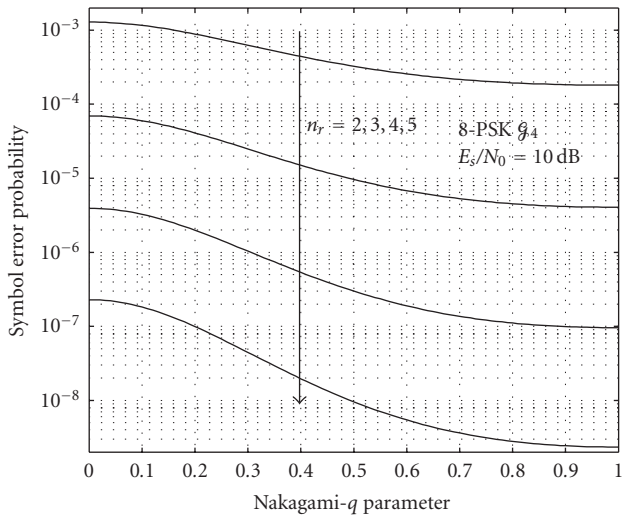

Figure 4: Symbol error probability of 8-PSK $\mathcal{G}_4$ in MIMO Nakagami-q fading channels as a function of the Nakagami-q parameter. $n_r = 2, 3, 4, 5$ and $E_s/N_0 = 10$ dB.

3 bits/s/Hz. From these two figures, we see that the analytical results match exactly with the simulation ones.

The effect of fading severity on the average SEP is illustrated in Figures 3 and 4 where the Nakagami-q parameter varies from 0 to 1. Figure 3 shows the average SEP of 8-PSK with L-branch MRC in SIMO Nakagami-q fading channels as a function of the Nakagami-q parameter when $L = 2, 3, 4, 5$ and $E_s/N_0 = 20$ dB. Similarly, Figure 3 shows the average SEP of 8-PSK $\mathcal{G}_4$ in MIMO Nakagami-q fading channels as a function of the q parameter when $n_r = 2, 3, 4, 5$ and $E_s/N_0 = 10$ dB. As the fading parameter q decreases—from the best case of Rayleigh fading ($q = 1$) to the worst case of one-sided Gaussian fading ($q = 0$)—we can clearly observe the increase in SEP due to more severe fading.

6. CONCLUSIONS

In this paper, we have derived the exact average SEP for a variety of binary and M-ary signals over SIMO and MIMO Nakagami-q fading channels with MRC and orthogonal space-time block coding, respectively. The final SEP expressions have been given generally in terms of Lauricella hypergeometric functions. Furthermore, it has been shown that the well-known results for Rayleigh fading are special cases of our final expressions.

APPENDIX

A. REDUCTION FORMULAS FOR $F_D^{(N)}$

Using Euler integral form of Lauricella hypergeometric function in (10), we can easily obtain two reduction formulas for $F_D^{(n)}$, which are useful in the paper, as follows.

(i) When $x_1 = x_2 = \cdots = x_m = x^\star$, $m \le n$,

$$F_D^{(n)}\left(a, \{b_i\}_{i=1}^n; c; \{x_i\}_{i=1}^n\right) = F_D^{(n-m+1)}\left(a, \sum_{i=1}^m b_i, \{b_i\}_{i=m+1}^n; c; x^\star, \{x_i\}_{i=m+1}^n\right). \tag{A.1}$$

(ii) When $b_n = -1$,

$$F_D^{(n)}\left(a, \{b_i\}_{i=1}^n; c; \{x_i\}_{i=1}^n\right) = F_D^{(n-1)}\left(a, \{b_i\}_{i=1}^{n-1}; c; \{x_i\}_{i=1}^{n-1}\right) - \frac{cx_n}{a} F_D^{(n-1)}\left(a+1, \{b_i\}_{i=1}^{n-1}; c+1; \{x_i\}_{i=1}^{n-1}\right). \tag{A.2}$$

ACKNOWLEDGMENTS

This research was supported by the Korean Science and Engineering Foundation (KOSEF) grant funded by the Korean government (MOST) (Grant no. R01-2007-000-11202-0).

REFERENCES

[1] M. K. Simon and M.-S. Alouini, "A unified approach to the performance analysis of digital communication over generalized fading channels," *Proceedings of the IEEE*, vol. 86, no. 9, pp. 1860–1877, 1998.

[2] M. K. Simon and M.-S. Alouini, *Digital Communication over Fading Channels: A Unified Approach to Performance Analysis*, Wiley-Interscience, New York, NY, USA, 2000.

[3] A. Annamalai and C. Tellambura, "Error rates for Nakagami-m fading multichannel reception of binary and M-ary signals," *IEEE Transactions on Communications*, vol. 49, no. 1, pp. 58–68, 2001.

[4] H. Shin and J. H. Lee, "On the error probability of binary and M-ary signals in Nakagami-m fading channels," *IEEE Transactions on Communications*, vol. 52, no. 4, pp. 536–539, 2004.

[5] G. P. Efthymogloua, T. Piboongungon, and V. A. Aalo, "Error rates of M-ary signals with multichannel reception in Nakagami-m fading channels," *IEEE Communications Letters*, vol. 10, no. 2, pp. 100–102, 2006.

[6] V. A. Aalo, T. Piboongungon, and G. P. Efthymoglou, "Another look at the performance of MRC schemes in Nakagami-*m* fading channels with arbitrary parameters," *IEEE Transactions on Communications*, vol. 53, no. 12, pp. 2002–2005, 2005.

[7] J. Lu, T. T. Tjhung, and C. C. Chai, "Error probability performance of *L*-branch diversity reception of MQAM in Rayleigh fading," *IEEE Transactions on Communications*, vol. 46, no. 2, pp. 179–181, 1998.

[8] C. Tellambura, A. J. Mueller, and V. K. Bhargava, "Analysis of *M*-ary phase-shift keying with diversity reception for land-mobile satellite channels," *IEEE Transactions on Vehicular Technology*, vol. 46, no. 4, pp. 910–922, 1997.

[9] N. Ekanayake, "Performance of *M*-ary PSK signals in slow Rayleigh fading channels," *Electronics Letters*, vol. 26, no. 10, pp. 618–619, 1990.

[10] H. Shin and J. H. Lee, "Performance analysis of space—time block codes over keyhole Nakagami-*m* fading chanels," *IEEE Transactions on Vehicular Technology*, vol. 53, no. 2, pp. 351–362, 2004.

[11] H. Shin and J. H. Lee, "Effect of keyholes on the symbol error rate of space—time block codes," *IEEE Communications Letters*, vol. 7, no. 1, pp. 27–29, 2003.

[12] H. Shin and M. Z. Win, "MIMO diversity in the presence of double scattering," to appear in *IEEE Transactions on Information Theory*, http://arxiv.org/abs/cs.IT/0511028.

[13] S. M. Alamouti, "A simple transmit diversity technique for wireless communications," *IEEE Journal on Selected Areas in Communications*, vol. 16, no. 8, pp. 1451–1458, 1998.

[14] V. Tarokh, H. Jafarkhani, and A. R. Calderbank, "Space—time block codes from orthogonal designs," *IEEE Transactions on Information Theory*, vol. 45, no. 5, pp. 1456–1467, 1999.

[15] D. A. Zogas, G. K. Karagiannidis, and S. A. Kotsopoulos, "Equal gain combining over Nakagami-*n* (Rice) and Nakagami-*q* (Hoyt) generalzied fading channels," *IEEE Transactions on Wireless Communications*, vol. 4, no. 2, pp. 374–379, 2005.

[16] G. Fraidenraich, J. C. S. S. Filho, and M. D. Yacoub, "Second-order statistics of maximal-ratio and equal-gain combining in Hoyt fading," *IEEE Communications Letters*, vol. 9, no. 1, pp. 19–21, 2005.

[17] N. Youssef, C.-X. Wang, and M. Pätzold, "A study on the second order statistics of Nakagami-Hoyt mobile fading channels," *IEEE Transactions on Vehicular Technology*, vol. 54, no. 4, pp. 1259–1265, 2005.

[18] R. M. Radaydeh, "Average error performance of *M*-ary modulation schemes in Nakagami-*q* (Hoyt) fading channels," *IEEE Communications Letters*, vol. 11, no. 3, pp. 255–257, 2007.

[19] H. Exton, *Multiple Hypergeometric Functions and Applications*, John Wiley & Sons, New York, NY, USA, 1976.

[20] A. Erdelyi, *Higher Transcendental Functions*, vol. 1, McGraw-Hill, New York, NY, USA, 1953.

[21] O. Tirkkonen and A. Hottinen, "Square-matrix embeddable space-time block codes for complex signal constellations," *IEEE Transactions on Information Theory*, vol. 48, no. 2, pp. 384–395, 2002.

[22] G. Fraidenraich and M. D. Yacoub, "The λ - μ general fading distribution," in *Proceedings of the SBMO/IEEE MTT-S International Microwave and Optoelectronics Conference (IMOC '03)*, vol. 1, pp. 49–54, Foz do Iguacu, Brazil, September 2003.

:: Open Access ::

EURASIP Journal on Embedded Systems

http://www.hindawi.com/journals/es/

Selected Papers from SLA++P 2007 Model-Driven High-Level Programming of Embedded Systems

Call for Papers

Model-based high-level programming of embedded systems has become a reality in the automotive and avionics industries. These industries place high demands on the efficiency and maintainabiliy of the design process as well as on the performance and functional correctness of embedded components. These goals are hard to reconcile in the face of the increasing complexity of embedded applications and target architecures that we see today. Research efforts towards meeting these goals have brought about a variety of high-level engineering design languages, tools, and methodologies. Their strength resides in clean behavioral models with strong semantical foundations providing a rigorous way to go from a high-level description to provable, that is, mathematically certifiable, executable code.

Undebatably, the most successful representatives of this trend of putting logic and mathematics behind design automation in embedded systems (known as Mike Fourman's "Lambda" programme) are synchronous languages. Firmly grounded in clean mathematical semantics, they have been receiving increasing attention in industry ever since they emerged in the 1980s. Lustre, Esterel, Signal are now widely and successfully used to program real-time and safety critical applications, from nuclear power plant management layer to Airbus air flight control systems. Their recent successes in the automatic control industry highlight the benefits of formal verification and automatic code generation from high-level models.

Model-based programming is making its way in other fields of software engineering, too, often involving cyclic synchronous paradigms. Strong interest is emerging in component programming for large-scale embedded systems, in the link between simulation tools and compiler tools, in languages for describing the system and its environment, integrated tools for both compilation and simulation of more general models of communication and coordination, and so on. The impact of such unifying methodologies will depend, among other things, on the extent to which it will be possible to maintain the high degree of predictability and verifiability of system behavior that is the strength of the classic synchronous world.

Topics of interest for this special issue cover, among others, the following:

- Synchronous programming formalisms
- Novel language paradigms blending synchrony with asynchrony and nondeterminism, discrete with continuous control
- Techniques for component abstraction and refinement
- New models of communication and coordination for embedded systems
- Model-based compilation and simulation techniques
- Specification, verification, and model-based testing
- Case-studies, industrial and teaching experiences

Submission to this special issue limited to the participants of the SLA++P conference who have been invited to submit to this issue.

Authors should follow the EURASIP Journal on Embedded Systems manuscript format described at the journal site http://www.hindawi.com/journals/es/. Prospective authors should submit an electronic copy of their complete manuscript through the journal Manuscript Tracking System at http://mts.hindawi.com/, according to the following timetable:

Manuscript Due	March 1, 2008
First Round of Reviews	June 1, 2008
Publication Date	September 1, 2008

Guest Editors

Florence Maraninchi, VERIMAG Laboratory, 38610 Gieres, France; florence.maraninchi@imag.fr

Michael Mendler, University of Bamberg, 96045 Bamberg, Germany; michael.mendler@wiai.uni-bamberg.de

Marc Pouzet, Laboratoire de Recherche en Informatique (LRI), Université Paris-Sud 11, 91405 Orsay Cedex, France; marc.pouzet@lri.fr

Hindawi Publishing Corporation
410 Park Avenue, 15th Floor, #287 pmb, New York, NY 10022, USA

HINDAWI

EURASIP Book Series on Signal Processing and Communications

UWB Communication Systems—A Comprehensive Overview

Edited by: Maria-Gabriella Di Benedetto,
Thomas Kaiser, Andreas F.Molisch, Ian Oppermann,
Christian Politano, and Domenico Porcino

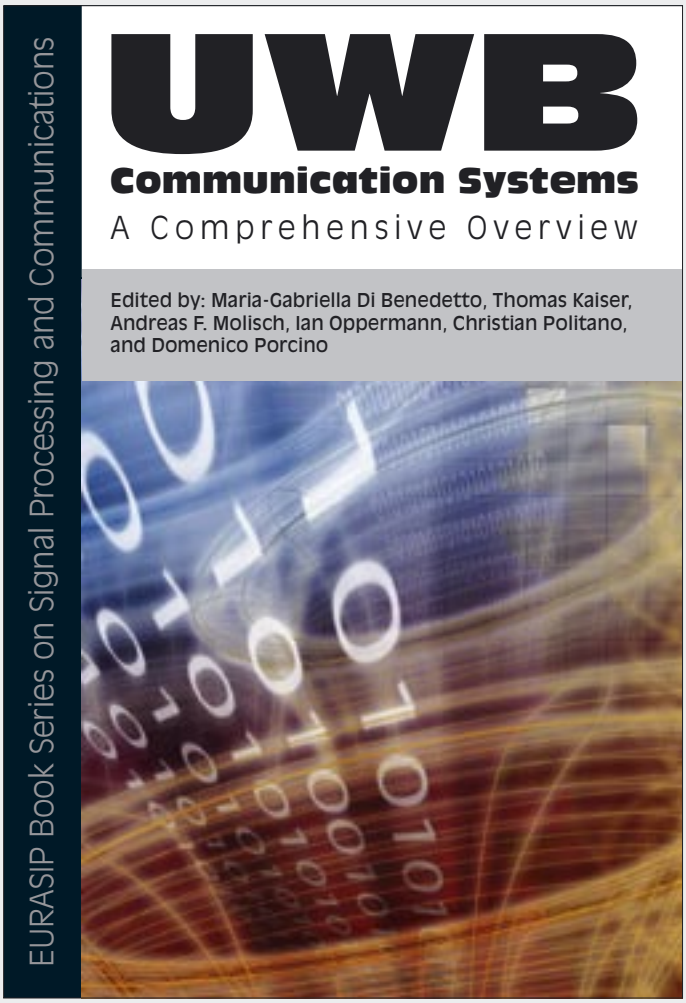

Ultrawideband (UWB) communication systems offer an unprecedented opportunity to impact the future communication world. The enormous available bandwidth, the wide scope of the data rate / range trade-off, as well as the potential for very low-cost operation leading to pervasive usage, all present a unique opportunity for UWB systems to impact the way people and intelligent machines communicate and interact with their environment.

The aim of this book is to provide an overview of the state of the art of UWB systems from theory to applications. Due to the rapid progress of multidisciplinary UWB research, such an overview can only be achieved by combining the areas of expertise of several scientists in the field. More than 30 leading UWB researchers and practitioners have contributed to this book covering the major topics relevant to UWB. These topics include UWB signal processing, UWB channel measurement and modeling, higher-layer protocol issues, spatial aspects of UWB signaling, UWB regulation and standardization, implementation issues, and UWB applications as well as positioning.

The book is targeted at advanced academic researchers, wireless designers, and graduate students wishing to greatly enhance their knowledge of all aspects of UWB systems.

EURASIP Book Series on SP&C, Volume 5, ISBN 977-5945-10-0
Please visit http://www.hindawi.com/spc.5.html for more information about the book. To place an order while taking advantage of our current promotional offer, please contact books.orders@hindawi.com